Electrochimica Acta 135 (2014) 121–127

Contents lists available at ScienceDirect

Electrochimica Acta

journal homepage: www.elsevier.com/locate/electacta

Titanate nanofibers sensitized with nanocrystalline Bi_2S_3 as new electrocatalytic materials for ascorbic acid sensor applications

J.F. Cabrita, V.C. Ferreira, O.C. Monteiro*

Centro de Química e Bioquímica, Faculdade de Ciências, Universidade de Lisboa, 1749-016 Lisboa, Portugal

ARTICLE INFO

Article history:
Received 20 December 2013
Received in revised form 14 March 2014
Accepted 23 April 2014
Available online 2 May 2014

Keywords:
Titanate nanofibers
Nanocrystalline Bi_2S_3
Electroactive nanocomposites
Ascorbic acid oxidation
Electrochemical sensors

ABSTRACT

Here is described a new method for titanate nanofibers (TNF) modification with nanocrystalline semiconducting bismuth sulphide (Bi_2S_3) nanoparticles in order to obtain new materials with innovative electrocatalytic properties. The TNF surface modification was achieved by *in situ* nucleation and growth of nanocrystalline metal sulphide particles through a single-source approach. Using bismuth diethyldithiocarbamate complex as the metal chalcogenide precursor, nanocrystalline of Bi_2S_3 particles were obtained over the TNF surface. The prepared materials were characterized and the results evidence that a thin layer of crystalline Bi_2S_3 nanosheets is covering the TNF' entire surface. After immobilization on a glassy carbon electrode, the nanocomposite structured surface was electrochemically characterized. The ability of the modified electrodes for sensor applications was tested towards the electrocatalysis for the ascorbic acid oxidation reaction. The results obtained indicate that these are very interesting materials to be used for sensing at pH 7, displaying a vitamin C linear response in the 1–10 mM concentration range.
© 2014 Elsevier Ltd. All rights reserved.

1. Introduction

L(+)-Ascorbic acid (AA, vitamin C) is the main antioxidant found in both animals and plants. For humans, AA is an essential nutrient due to its participation in several metabolic reactions. Consequently it has been widely used in foods, beverages and pharmaceutical products [1–4].

For diagnostic and food safety applications, the development of a simple and rapid method for AA determination with high selectivity and sensitivity is desirable. AA analytical quantification has been reported by many methodologies, such as enzymatic [5], chromatographic [6], fluorimetric [7] and electrochemical methods [8–11]. Among them, electrochemical sensing has proven to be an inexpensive and simple analytical method with remarkable detection sensitivity, reproducibility, low detection limits, and liable of miniaturization [12]. The use of nanoparticles modified electrodes have been described as a very promising route for electrochemical AA sensor fabrication [13–15]. Recently, poly(xanthurenic acid) and multi-walled carbon nanotubes hybrid composite [16] and nitrogen doped graphene [17], have been reported as interesting advanced electrode materials for AA electrochemical sensing. Simultaneously an electrochemical ascorbic acid sensor was also successfully achieved using a glassy carbon electrode modified with palladium nanoparticles supported on graphene oxide [18].

Among the nanotubular materials that have been synthesised during the last two decades, titanate nanostructures have attracted increasing attention in recent years [19–22]. By conveniently combining the properties of TiO_2 nanoparticles with the ones of layered titanates, wide potential applicability of the TNF can be envisaged, including photocatalysis [23], as substrate to different active catalysts decoration [24], dye-sensitized solar cells [25], and sensors [26]. TNF has been proven to be an attractive matrix to immobilize and study the redox process of biomolecules, *e.g.* myoglobin, showing potentialities to be incorporated in the third generation of biosensor devices [27]. The use of titanate nanotubes as direct electron transfer promoter in order to develop an electrochemical biosensor for lactate detection has also been described [28].

Semiconducting bismuth sulfide (Bi_2S_3) is an important member of V-VI group and it is a direct band gap material ($E_g = 1.2$ eV). Nanocrystalline particles of this material have been described for several optical [29] and electrochemical applications [30–32]. The preparation of nanocrystalline Bi_2S_3 particles have been reported using several methods [33–38]; lamellar particles with enhanced adsorbent and photocatalytic properties have been described by a single-source approach using bismuth(III) dialkyl-dithiocarbamate as the Bi_2S_3 precursor [29]. Surface-modified Bi_2S_3 urchin-like nanospheres have been intensively investigated for electrochemical DNA detection analysis [39]. A simple electrochemical method based on a Bi_2S_3 modified glassy carbon electrode was successfully

* Corresponding author. Tel.: +351 217500865; fax: +351 217500088.
E-mail address: ocmonteiro@fc.ul.pt (O.C. Monteiro).

http://dx.doi.org/10.1016/j.electacta.2014.04.135
0013-4686/© 2014 Elsevier Ltd. All rights reserved.

used to determine antipyrine in pharmaceutical formulations [40]. Furthermore, electrochemical measurements show that hierarchical Bi_2S_3 architectures can display high electrochemical hydrogen storage and electrochemical Li^+ intercalation ability [41].

In this work, the preparation, by synergeticallly combining nanocrystalline lamellar Bi_2S_3 and TNF, of a new nanocomposite structured material with improved electrochemical sensor properties was aimed. A swift synthesis approach was used to prepare homogeneous and stable titanate nanofibers and afterwards a single-source approach was employed to accomplish the Bi_2S_3 sensitization. After structural and morphological characterization, the nanocomposite materials were successfully immobilized in a glassy carbon electrode and the modified, and very stable, surface was used as catalyst for the AA oxidation reaction. The results indicate that the Bi_2S_3/TNF nanocomposite is a very promising material for surface modification, which exhibits high electrocatalytic activity towards the AA oxidation reaction, enhanced stability, displaying a linear response for the AA concentrations in the 1–10 mM range.

2. Experimental

2.1. Materials and Methods

All reagents were of analytical grade (Aldrich and Fluka) and were used as received. The solutions were prepared with Millipore Milli-Q ultra-pure water.

2.1.1. TNF precursor synthesis

The TNF precursor was prepared using a reported procedure [42]. A titanium trichloride solution (10 wt.% in 20-30 wt.% HCl) diluted in a ratio of 1:2 in standard HCl solution (37%) was used as the titanium source. A 4 M ammonia aqueous solution ($\sim$ 350 mL) was added drop-wise to this solution, under vigorous stirring, until complete precipitation of a white solid. The obtained suspension was kept overnight at room temperature and then filtered and vigorously rinsed with deionised water in order to remove the remaining ammonium and chloride ions.

2.1.2. TNF synthesis

Synthesis of the TNF samples was performed in an autoclave system using 6 g of precursor in *ca.* 60 ml of NaOH 10 M aqueous solution. Samples were prepared at 200 °C, using an autoclave dwell time of 12 hours. After cooling, the samples were washed with water until pH 7 was reached on the filtrate solution. After being washed the solid was dried and stored.

2.1.3. Bi_2S_3 precursor synthesis

The metal chalcogenide precursor, $\{Bi_2[S_2CN(C_2H_5)_2]_3\}$, was prepared as previously reported [43]: 40 mmol of the diethylamine and 50 mmol of carbon disulphide were added to a suspension containing 6 mmol of bismuth(III) oxide in methanol (20 mL). The mixture was stirred over 24 h and a yellow solid was obtained. The solid was crystallized in hot chloroform/methanol (3:1); the Bi(III) complex was identified by IR spectroscopy.

2.1.4. TNF sensitization

The Bi_2S_3/TNF nanocomposite particles were prepared by adding drop-wise ethylenediamine (2.5 mL) to an $\{Bi_2[S_2CN(C_2H_5)_2]_3\}$ acetone solution (0.125 mmol; 50 mL) containing 0.250 g of TNF particles [29]. The suspension formed was then refluxed with stirring during four hours. The obtained dark grey solid was collected by centrifugation, washed with acetone and dried at room temperature in a desiccator over silica gel.

2.1.5. Bi_2S_3 nanocrystals synthesis

The semiconductor nanocrystalline particles were prepared using the procedure described above (Section 2.1.4) without the presence of the TNF particles.

2.2. Characterization

X-ray powder diffraction was performed in a Philips X-ray diffractometer (PW 1730) with automatic data acquisition (APD Philips v3.6B), and a Cu Kα radiation (λ = 0.15406 nm) and working at 40 kV/30 mA. The diffraction patterns were collected in the range 2θ = 7-60°, with a 0.02° step size and an acquisition time of 2.0 s/step. Transmission electron microscopy (TEM and HRTEM) was carried out in a JEOL 200CX microscope operating at 200 kV.

The electrochemical experiments were carried out in a computer-controlled CHI620A electrochemical workstation using a conventional three-electrode cell, using a platinum foil as counter electrode and a saturated calomel electrode (SCE) as reference electrode. All potentials are reported with respect to the SCE. The redox potential of the SCE is +0.244 V *vs.* SHE at 25 °C. The working electrode used was a glassy carbon electrode (GCE, geometric area A_{GCE} = 0.57 cm^2). Before each experiment the GCE was hand-polished in aqueous suspensions of successively finer grades of alumina (from 5 down to 0.3 μm), until a mirror-finishing surface was obtained; subsequently, copiously rinsed with Millipore-Q water and then dried using a N_2 flow.

The GCE surface was modified with the TNF, Bi_2S_3 (bulk and nanoparticles) or Bi_2S_3/TNF samples. The immobilization was performed by a drop-cast methodology, typically 30 μL of a 1 mg mL^{-1} suspension (52.6 μg cm^{-2}), overnight, to allow slowly solvent evaporation, resulting in a uniform coverage of the GCE surface. Fast dry of the TNF suspension resulted in poorly attached material to the GCE surface, whilst the experimental circumstances employed here (i.e. slow overnight drying) ensures stable attachment of the TNF, Bi_2S_3/TNF and Bi_2S_3 particles to the surface and no detachment of materials was observed during the time of the experiments. No other thermal treatment was performed before electrochemical characterization.

The electrocatalytic performance of the CGE surfaces, before and after Bi_2S_3/TNF film coating, towards the AA oxidation in a 0.1 M phosphate buffer solution (PBS) was evaluated by cyclic voltammetry (E = [-0.40 to +0.80] V *vs.* SCE with a scan rate of 0.05 V s^{-1}) and by chronoamperometric measurements (successive injections of AA) at a working potential of +0.25 V *vs.* SCE.

3. Results and discussion

3.1. Decorated Bi_2S_3/TNF characterization

After preparation at 200 °C during 12 hours, the TNF were analysed by XRD. As can be seen in Fig. 1, the diffraction peaks at 2θ = 10.6°, 24.5°, 28.6° and 48.6° are in agreement with the existence of material with a titanate layered structure, type $Na_2Ti_3O_7$ [42]. After treatment with $[Bi_2(S_2CN(C_2H_5)_3]$, the TNF sample was also characterized by XRD. The obtained XRD pattern (Fig. 1) indicates the presence of a second semiconductor crystalline phase on the Bi_2S_3/TNF sample, and this is in accordance with the nanocrystalline structure of Bi_2S_3 *bismuthinite* (JCPDS file 17-0320). Nevertheless the undoubted identification of this new phase was difficult only by using the XRD data since the peaks are broaden and poorly defined. In order to overcome this problem, samples of nanocrystalline Bi_2S_3 powder were also prepared (sample nanoBi_2S_3). The presence of nanocrystalline Bi_2S_3, in the Bi_2S_3/TNF sample, was accomplished by comparing the XRD patterns of the

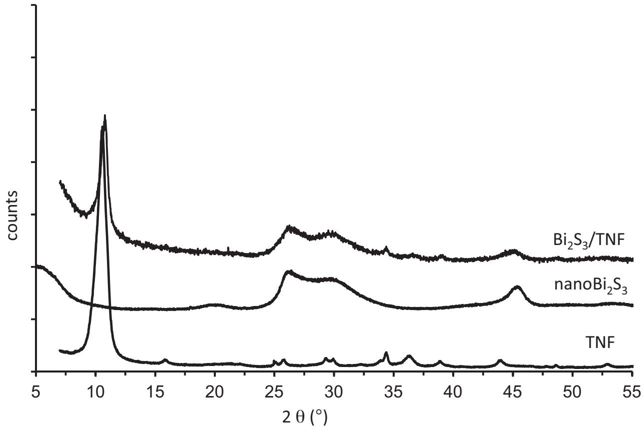

Fig. 1. XRD patterns of the TNF, Bi_2S_3/TNF and nanoBi_2S_3 powders.

TNF sample, before and after Bi_2S_3 sensitization, with the one of the nanoBi_2S_3 powder.

The morphology of the decorated Bi_2S_3/TNF powder was analysed by transmission electron microscopy (TEM). From the micrographs shown in Fig. 2a it can be seen that the TNF sample, prior to sensitization, is morphologically homogeneous and comprises thin elongated nanostructures with a high length/diameter aspect ratio. Fig. 2b shows a image of the Bi_2S_3/TNF nanocomposite sample, showing Bi_2S_3 nanocrystals, with sheet-like network morphology, grown at the TNF surface. No evidence of segregation of secondary phases was observed. A TEM image of the nanoBi_2S_3 sample is also presented for comparative purposes. This powder presents also a sheet-like network morphology although in this case the formation of spherical agglomerates is clearly seen (Fig. 2c). The Bi_2S_3 thin sheet-like morphology, covering completely the TNF surface, was confirmed by a close inspection using HRTEM (Fig. 2b - inset).

The EDS analysis performed over one Bi_2S_3/TNF single particle showed peaks for Bi and S, as well for Ti and Na. These peaks can be related with the existence of Bi_2S_3 and TNF in the nanocomposite material; being this result in agreement with the existence of Bi_2S_3 nanosheets over the TNF surface.

3.2. Bi_2S_3/TNF electrochemical characterization

The combination of titanate nanofibers with nanocrystalline lamellar Bi_2S_3 to construct new electro-active composite architectures, for instance for sensor applications, is a very interesting research subject. Based on this and on previous published results concerning the catalytic activity of nanocrystalline Bi_2S_3 based materials [29,44,45], the Bi_2S_3/TNF sample was evaluated for the catalytic ascorbic acid oxidation reaction, considering the possibility of future sensor applications.

The overall reaction of the AA oxidation can be expressed by the following equation:

$$C_6H_8O_6 \rightarrow 2H^+ + 2e^- + C_6H_6O_6$$

(ascorbic acid) (dehydroascorbate)

Fig. 3 shows the electrochemical characterization of the GCE electrodes before and after modification with Bi_2S_3/TNF, in the absence and in the presence of 1 mM ascorbic acid in buffer medium at pH 7 (PBS). The GCE electrode is electroactive for the AA irreversible oxidation reaction, with an oxidation peak occurring at +0.37 V. Upon modification with Bi_2S_3/TNF a significant potential shift towards less positive values (*ca.* 63 mV) is visualized and attributed to the electrocatalytic activity of the Bi_2S_3/TNF towards the AA oxidation reaction. Thus, confirming that the

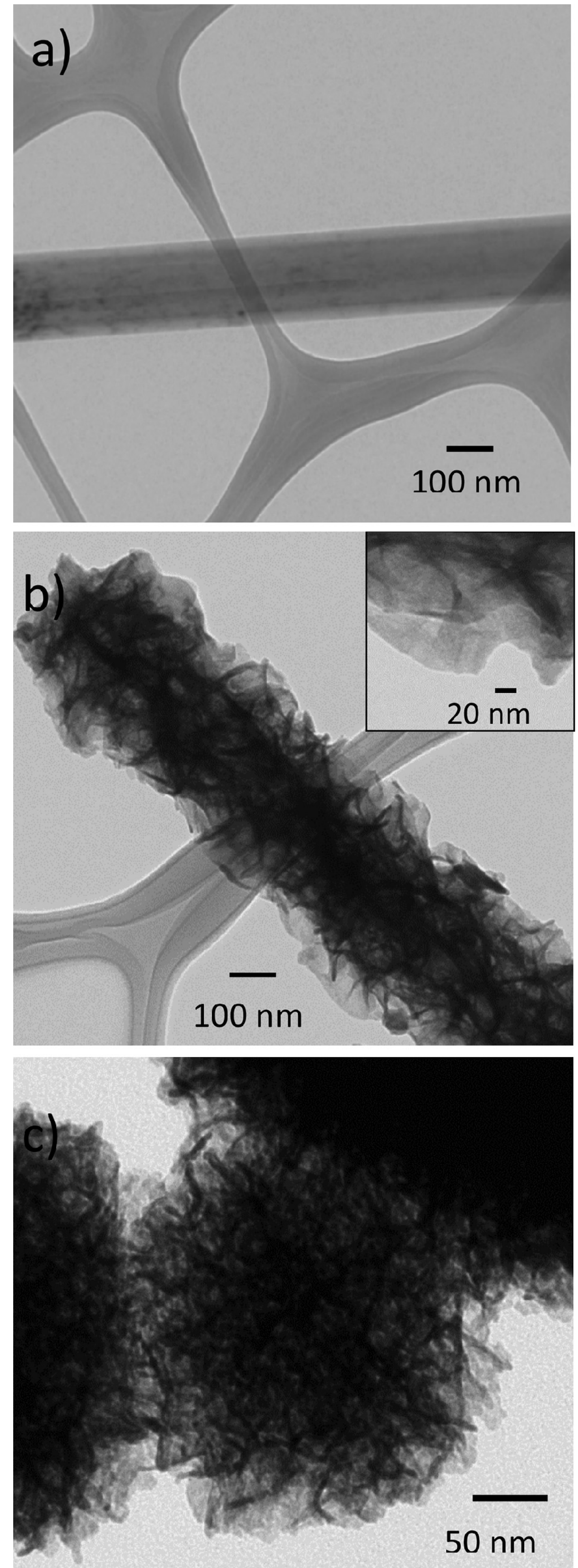

Fig. 2. TEM images of the TNF (a), Bi_2S_3/TNF (b) and nanoBi_2S_3 (c) samples. Inset in (b): Bi_2S_3/TNF detail.

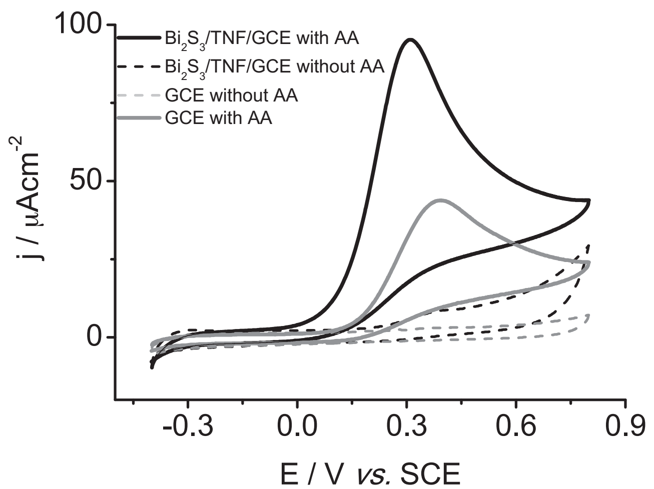

Fig. 3. Cyclic voltammograms of the GCE and Bi_2S_3/TNF/GCE modified electrodes in a 0.1 M PBS, pH 7 solution; $\nu = 50\,mV\,s^{-1}$.

nanocomposite Bi_2S_3/TNF film, deposited on the GCE surface, catalyzes the AA oxidation, better than the GCE surface itself.

Under the employed experimental conditions, the higher AA oxidation current density observed for the nanocomposite, as compared with the one for GCE electrode (95.20 and 43.40 $\mu A\,cm^{-2}$, respectively) could be attributed, in a preliminary analysis, to the increased surface area conferred by the presence of the Bi_2S_3/TNF. In order to clarify this point, the GCE surface was also modified with identical amounts of TNF, nanocrystalline Bi_2S_3 (nanoBi_2S_3 sample) and bulk Bi_2S_3 particles (bulkBi_2S_3 sample). The electrochemical performance of these modified electrodes, evaluated in the presence of AA under identical conditions, as depicted in Fig. 4 and the results summarized in Table 1. Additionally, these experiments allow also to assign the nanocomposite catalytic activity of each of the Bi_2S_3/TNF components and to study the influence of the particle size on the Bi_2S_3 electrochemical response.

Apart from the Bi_2S_3/TNF/GCE material, no enhanced electrocatalytic activity, towards the studied reaction, was found with any other of the tested modified electrodes: nanoBi_2S_3, bulkBi_2S_3 and TNF. It is interesting to note that, in spite of the increased surface area, the AA oxidation current density is lower for these modified surfaces when compared with the GCE surface, suggesting an electric blocking effect produced by the semiconductors presence over the electrode surface. These results indicate that the Bi_2S_3/TNF/GCE electrocatalytic activity is a result of the synergetic combination of the nanocrystalline Bi_2S_3 with the TNF particles. Moreover, taking into account the results obtained, it is reasonable to assume that

Table 1
$E_{p\,ox.}$ and $j_{ox.}$ experimental values obtained for the different modified electrodes.

Modified electrode	[AA]/mM	pH	$E_{pox.}$/V	$j_{ox.}$/$\mu A\,cm^{-2}$
GCE	1	7	0.37	43.4
Bi_2S_3/TNF/GCE			0.31	95.2
TNF/GCE			0.42	36.4
nanoBi_2S_3/GCE			0.39	27.8
bulkBi_2S_3/GCE			0.39	27.5
Bi_2S_3/TNF/GCE	1	4	0.42	172.7
		10	0.66	40.0
Bi_2S_3/TNF/GCE	0.1	7	0.34	6.4
	0.5		0.37	23.6
	1		0.31	97.1
	5		0.39	461.5
	10		0.43	766.2

the higher current density observed at the Bi_2S_3/TNF/GCE surface, outcomes from the combination of the nanostructured materials properties in the composite and is not a surface area effect, since the same behavior was not detected for the other samples with identical/superior surface area.

3.2.1. Effect of experimental parameters

In order to evaluate the pH range applicability of the Bi_2S_3/TNF/GCE modified surface, experiments using pH = 4, 7 and 10 were carried out. According to literature, the pKa of AA is near 4.17 and 11.57 [46]. At pH= 4, the AA molecules are expected to be in their neutral form and for pH higher than 4.17 the AA molecules will possess a negative charge due to the protons loss.

Although TNF are well known by their ability to adsorb cationic dyes from solution [19,21,47], those are not expected to increase the electrochemical response towards the AA oxidation through an adsorption effect since in the pH range used the AA is in its anionic form (pKa = 4.17) as ascorbate anion, and the TNF prepared under the experimental conditions employed here present a negatively charged surface (p.z.c ~ 3.1) [23]. In fact, the possibility of acid ascorbic acid adsorption in the TNF and Bi_2S_3 surfaces was experimental evaluated and no adsorption occurs.

The cyclic voltammograms (CV) recorded for the Bi_2S_3/TNF/GCE modified electrode in the presence of AA, in solutions with the different pH values are presented in Fig. 5. As reported, the voltammetric response is strongly pH dependent [48,49]. The peak current density from the electrocatalytic oxidation of AA in acid solution (pH 4) is higher than that in neutral (pH 7) or alkaline conditions (pH 10). The highest current density was observed using the Bi_2S_3/TNF/GCE modified surface under pH 4. However and apart from the AA redox behavior a small oxidation peak at -0.1 V is visible for this medium. This peak is due to the Bi_2S_3/TNF existence over the GCE surface since it is also visible in a CV recorded using

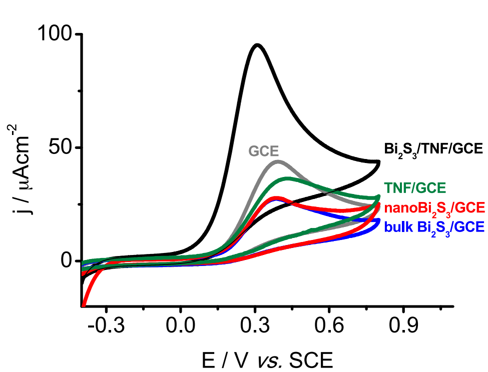

Fig. 4. Cyclic voltammograms of the GCE, TNF/GCE, Bi_2S_3/TNF/GCE, nanoBi_2S_3/GCE and bulkBi_2S_3/GCE modified electrodes in a 1 mM AA solution, in PBS pH 7; $\nu = 50\,mV\,s^{-1}$.

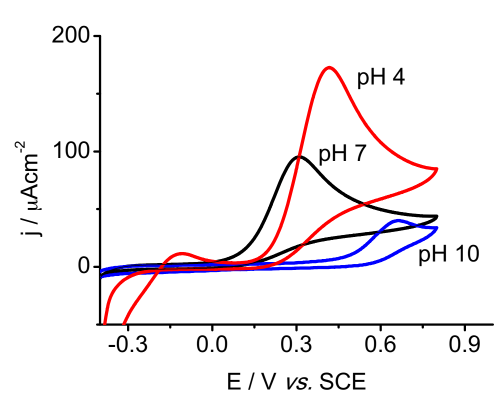

Fig. 5. Cyclic voltammograms of the Bi_2S_3/TNF/GCE modified electrode in 1 mM AA solutions with different pH values.

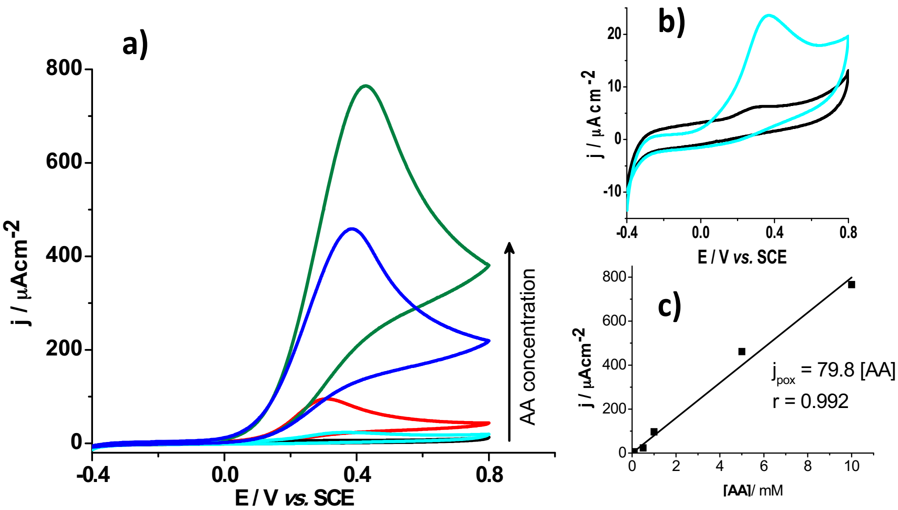

Fig. 6. (a) Cyclic voltammograms of the Bi_2S_3/TNF/GCE modified electrode; 0.1 M PBS solution (pH 7) with different AA concentration (0.1, 0.5, 1, 5 and 10 mM); ν = 50 mV s^{-1}; (b) detail of the CV of the Bi_2S_3/TNF/GCE modified electrode for the 0.1 and 0.5 mM AA; (c) relationship between current density and AA concentration in solution.

an electrolyte solution without AA, at the same pH. No similar oxidation peak was observed for pH 7 and pH 10. At pH 10, the AA oxidation occurs at a higher potential (~ 0.66 V) and with the lowest current density, comparatively to pH 7 and pH 4 experiments. These results are in agreement with previous works [12] and are attributed to the AA instability in alkaline media.

The AA oxidation peak potential shifts towards more negative potential values (~ 0.31 V) for pH 7 and the current density is higher (95 μA cm^{-2}) than the one found for pH 10.

To study the effect of the AA concentration in the Bi_2S_3/TNF/GCE electro-catalytic response, experiments using 0.1-10 mM AA solutions were performed (Fig. 6). As can be seen, the anodic peak current density linearly increases with the AA concentration and the oxidation peak potential shifts to higher values. For the Bi_2S_3/TNF/GCE modified electrode, a linear relationship was found between the AA concentration and the current density. The increase observed in the current density with the AA concentration indicates that the modified electrode possess good sensitivity and stability in the AA presence. This novel Bi_2S_3/TNF film modified GCE demonstrated to be an efficient electrocatalyst towards the AA oxidation in a broader concentration range (0.1–10 mM) regarding other systems reported in the literature [9,50–52]. For the reaction under study, a graphene modified GCE sensor proved to have good electrocatalytic response over the same concentration range, however, besides AA oxidation occurred at less positive potentials the correspondent catalytic currents were much lower than the ones observed in the present work [11].

To study the AA oxidation reaction kinetics, over the Bi_2S_3/TNF/GCE surface, CVs were recorded at different scan rates as shown in Fig. 7. The plot of peak current *vs.* scan rate showed linearity with good correlation (inset - Fig. 7). The linear increase of the anodic peak current with the scan rate indicates fast charge transfer between AA and the modified electrode. Moreover, the linearity between the anodic peak current with the square root of the scan rate reveals a diffusional controlled mass transport process. No specific studies were performed on the stability of the films but during the experimental work no detachment of the films or

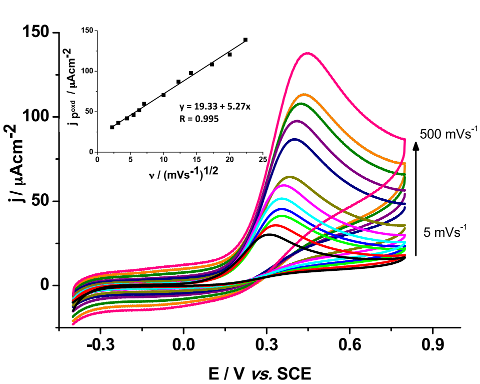

Fig. 7. Cyclic voltammograms of the Bi_2S_3/TNF/GCE modified surface in 1 mM AA solution, at pH 7, using different scan rates. Inset: relationship between oxidation peak current and scan rate.

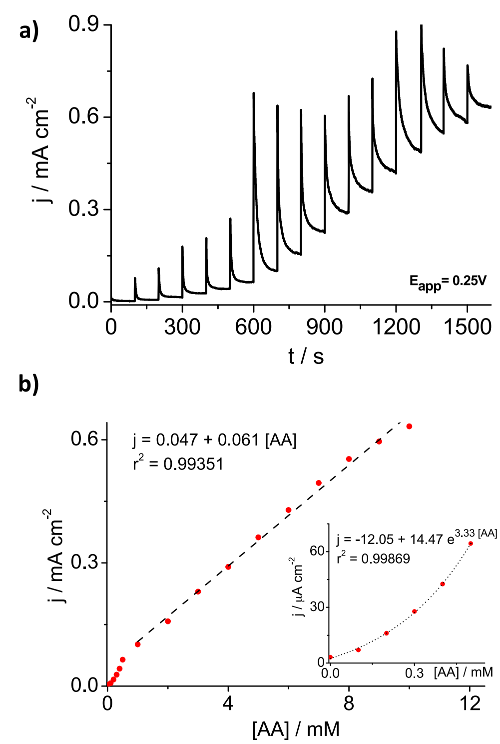

Fig. 8. (a) Amperometric curve i *vs.* t of Bi_2S_3/TNF/GCE, in a stirring 0.1 M PBS pH 7 solution, at +0.25 V, for successive additions of 0.1-0.5 and 1-10 mM AA; (b) relationship between current density and AA concentration. Inset: detail of the 0.1-0.5 mM AA range.

significant loss of activity were visualized during several consecutive runs (sometimes more than 30).

3.3. Bi_2S_3/TNF/GCE amperometric response

The amperometric determination of AA using the Bi_2S_3/TNF/GCE modified electrode was studied *via* successive injections of Vitamin C aliquots (0.1–10 mM) to an AA stirring solution (0.1 M PBS, pH 7), under an applied potential of +0.25 V. Fig. 8 depicts the Bi_2S_3/TNF/GCE amperometric response obtained upon the AA injections. As can be observed, for AA concentrations lower than 1 mM a quasi-exponential behavior was observed for the Bi_2S_3/TNF/GCE modified electrode surface response. A linear fit of the amperometric signal was observed for AA concentrations between 1 and 10 mM, with a sensitivity of 38 $\mu A\,mM^{-1}\,cm^{-2}$, indicating that the Bi_2S_3/TNF/GCE surface has a high potential to be used for AA sensor applications in this concentration range.

Experimental work related with the use of Bi_2S_3/TNF/GCE modified surfaces for determination of AA in the presence of interfering species is now in progress.

4. Conclusions

Crystalline Bi_2S_3/TNF nanocomposite materials were successfully obtained by a new synthesis methodology. Through XRD and TEM characterization, nanocrystalline thin sheets of Bi_2S_3 covering the entire TNF surface were observed for the new Bi_2S_3/TNF material. A higher catalytic activity for the AA oxidation reaction was observed for the Bi_2S_3/TNF/GCE modified surface, when compared with the GCE, TNF, nanocrystalline and bulk Bi_2S_3 particles. The best pH medium found was pH 7. A sensitivity of 38 $\mu A\,mM^{-1}\,cm^{-2}$, along with high stability and a linear response of the Bi_2S_3/TNF/GCE were observed for the AA amperometric determination in the 1–10 mM range. These results show that Bi_2S_3/TNF materials have electrocatalytic activity towards AA oxidation, are stable and can be seen as promising materials for future AA sensor devices fabrication.

Acknowledgments

The authors thank Fundação para a Ciência e Tecnologia (FCT) for financial support (PTDC/CTM-NAN/113021/2009, SFRH/BPD/77404/2011 and PEst-OE/QUI/UI0612/2013).

References

[1] P.A. Kilmartin, A. Martinez, P.N. Bartlett, Polyaniline-based microelectrodes for sensing ascorbic acid in beverages, Current Appl. Phys. 8 (2008) 320–323.
[2] S. Ivanov, V. Tsakova, V.M. Mirsky, Conductometric transducing in electrocatalytical sensors: detection of ascorbic acid, Electrochem. Commun. 8 (2006) 643–646.
[3] D. Ragupathy, A.I. Gopalan, K.-P. Lee, K.M. Manesh, Electro-assisted fabrication of layer-by-layer assembled poly(2,5-dimethoxyaniline)/phosphotungstic acid modified electrode and electrocatalytic oxidation of ascorbic acid, Electrochem Commun. 10 (2008) 527–530.
[4] A.G. Frenich, M.E.H. Torres, A.B. Vega, Determination of ascorbic acid and carotenoids in food commodities by liquid chromatography with mass spectrometry detection, J. Agri. Food Chem. 53 (2005) 7371–7376.
[5] W. Lee, S.M. Roberts, R.F. Labbe, Ascorbic acid determination with an automated enzymatic procedure, Clin. Chem. 43 (1997) 154–157.
[6] A. Tai, E. Gohda, Determination of ascorbic acid and its related compounds in foods and beverages by hydrophilic interaction liquid chromatography, J. Chromatogr. B 853 (2007) 214–220.
[7] X. Wu, Y. Diao, C. Sun, J. Yang, Y. Wang, S. Sun, Fluorimetric determination of ascorbic acid with *o*-phenylenediamine, Talanta 59 (2003) 95–99.
[8] S.M. Chen, J.Y. Chen, V.S. Vasantha, Electrochemical preparation of epinephrine/Nafion chemically modified electrodes and their electrocatalytic oxidation of ascorbic acid and dopamine, Electrochim. Acta 52 (2006) 455–465.
[9] D. Ragupathy, A.I. Gopalan, K. Lee, Electrocatalytic oxidation and determination of ascorbic acid in the presence of dopamine at multiwalled carbon nanotube-silica network-gold nanoparticles based nanohybrid modified electrode, Sens. Actuators B 143 (2010) 696–703.
[10] J. Wang, S. Yang, D. Guo, P. Yu, D. Li, J. Ye, L. Mao, Comparative studies on electrochemical activity of graphene nanosheets and carbon nanotubes, Electrochem. Commun. 11 (2009) 1892–1895.
[11] D.V. Stergiou, E.K. Diamanti, D. Gournis, M.I. Prodromidi, Comparative study of different types of graphenes as electrocatalysts for ascorbic acid, Electrochem. Commun. 12 (2010) 1307–1309.
[12] S. Chairam, W. Sriraksa, M. Amatatongchai, E. Somsook, Electrocatalytic oxidation of ascorbic acid using a poly(aniline-*co*-*m*-ferrocenylaniline) odified glassy carbon electrode, Sensors 11 (2011) 10166–10179.
[13] K.-P. Lee, A.I. Gopalan, P. Santhosh, K.M. Manesh, J.H. Kim, K.S. Kim, Fabrication and electrocatalysis of self-assembly directed gold nanoparticles anchored carbon nanotubes modified electrode, J. Nanosci. Nanotechnol. 6 (2006) 1575–1583.
[14] A. Ambrosi, A. Morrin, M.R. Smyth, A.J. Killard, The application of conducting polymer nanoparticle electrodes to the sensing of ascorbic acid, Anal. Chim. Acta 609 (2008) 37–43.
[15] J. Huang, Y. Liu, H. Hou, T. You, Simultaneous electrochemical determination of dopamine, uric acid and ascorbic acid using palladium nanoparticle-loaded carbon nanofibers modified electrode, Biosens. Bioelectron. 24 (2008) 632–637.
[16] K. Lin, P. Yeh, S. Chen, Electrochemical determination of ascorbic acid using poly(xanthurenic acid) and multi-walled carbon nanotubes, Int. J. Electrochem. Sci. 7 (2012) 12752–12763.
[17] Z. Sheng, X. Zheng, J. Xu, W. Bao, F. Wang, X. Xia, Electrochemical sensor based on nitrogen doped graphene: Simultaneous determination of ascorbic acid, dopamine and uric acid, Biosens. Bioelectron. 34 (2012) 125–131.
[18] G. Wu, Y. Wu, X. Liu, M. Rong, X. Chen, X. Chen, An electrochemical ascorbic acid sensor based on palladium nanoparticles supported on graphene oxide, Anal. Chim. Acta 745 (2012) 33–37.
[19] D.V. Bavykin, F.C. Walsh, Elongated titanate nanostructures and their applications, Eur. J. Inorg. Chem. 8 (2009) 977–997.
[20] H.-H. Ou, S.-L. Lo, Review of titania nanotubes synthesized via the hydrothermal treatment: fabrication, modification, and application, Sep. Purif. Technol. 58 (2007) 179–191.
[21] D.V. Bavykin, F.C. Walsh, Titanate and titania nanotubes: synthesis, Cambridge, properties and applications, RSC, 2010.
[22] N. Liu, X. Chen, J. Zhang, J.W. Schwank, A review on TiO_2-based nanotubes synthesized via hydrothermal method: Formation mechanism, structure modification, and photocatalytic applications, Catal. Today 225 (2014) 34–51.
[23] V. Bem, M.C. Neves, M.R. Nunes, A.J. Silvestre, O.C. Monteiro, Influence of the sodium/proton replacement on the structural, morphological and photocatalytic properties of titanate nanotubes, J Photochem. Photobio. A 232 (2012) 50–56.
[24] M.W. Xiao, L.S. Wang, Y.D. Wu, X.J. Huang, Z. Dang, Preparation and characterization of CdS nanoparticles decorated into titanate nanotubes and their photocatalytic properties, Nanotechnology 19 (2008) 015706–015712.
[25] S. So, K. Lee, P. Schmuki, Ru-doped TiO_2 nanotubes: improved performance in dye-sensitized solar cells, Phys. Stat. Sol. RRL 6 (2012) 169–171.
[26] Y. Kwon, H. Kim, S. Lee, I.-J. Chin, T.-Y. Seong, W.I. Lee, C. Lee, Enhanced ethanol sensing properties of TiO_2 nanotube sensors, Sens. Actuators B 173 (2012) 441–446.
[27] A. Liu, M. Wei, I. Honma, H. Zhou, Direct electrochemistry of myoglobin in titanate nanotubes film, Anal Chem. 77 (2005) 8068–8074.
[28] M. Yang, J. Wang, H. Li, J. Zheng, N. NickWu, A lactate electrochemical biosensor with a titanate nanotube as direct electron transfer promoter, Nanotechnology 19 (2008) 075502–075507.
[29] R. Albuquerque, M.C. Neves, M.H. Mendonça, T. Trindade, O.C. Monteiro, Adsorption and catalytic properties of SiO_2/Bi_2S_3 nanocomposites on the methylene blue photodecolorization process Colloids Surf. A: Physicochem, Eng. Aspects 328 (2008) 107–113.
[30] R.R. Ahire, N.G. Deshpande, Y.G. Gudage, A.A. Sagade, S.D. Chavhan, D.M. Phase, R. Sharma, A comparative study of the physical properties of CdS, Bi_2S_3 and composite CdS–Bi_2S_3 thin films for photosensor application, Sens. Actuators 140 (2007) 207–214.
[31] J. Ma, Z. Liu, J. Lian, X. Duan, T. Kim, P. Peng, X. Liu, Q. Chen, G. Yao, W. Zheng, Ionic liquids-assisted synthesis and electrochemical properties of Bi_2S_3 nanostructures, CrystEngComm 13 (2011) 3072–3079.
[32] Q.X. Wang, F. Gao, S.X. Li, W. Weng, Z.S. Hu, Preparation of cauliflower-like bismuth sulfide and its application in electrochemical sensor, Chinese Chem. Lett. 19 (2008) 585–588.
[33] C. Ye, G. Meng, Z. Jiang, Y. Wang, G. Wang, L. Zhang, Rational growth of Bi_2S_3 nanotubes from quasi-two dimensional precursors, J. Am. Chem. Soc. 124 (2002) 15180–15181.
[34] M.B. Sigman Jr., B.A. Korgel, Solventless synthesis of Bi_2S_3 (*bismuthinite*) nanorods nanowires, and nanofabric, Chem. Mater. 17 (2005) 1655–1660.
[35] X.S. Peng, G.W. Meng, J. Zhang, L.X. Zhao, X.F. Wang, Y.W. Wang, L.D. Zhang, Electrochemical fabrication of ordered Bi_2S_3 nanowire arrays, J. Phys. D: App. Phys. 34 (2001) 3224–3228.
[36] Z.P. Liu, J.B. Liang, S. Li, S. Peng, Y.T. Qian, Synthesis and growth mechanism of Bi_2S_3 nanoribbons, Eur. J. Chem. 10 (2004) 634–640.
[37] J. Jiang, S.H. Yu, W.T. Yao, H. Ge, G.Z. Zhang, Morphogenesis and crystallization of Bi_2S_3 nanostructures by an ionic liquid-assisted templating route: synthesis, formation mechanism and properties, Chem. Mater. 17 (2005) 6094–6100.

[38] P.K. Panigrahi, A. Pathak, The growth of bismuth sulfide nanorods from spherical-shaped amorphous precursor particles under hydrothermal condition, J.Nanopart. 2013 (2013) 1–11.

[39] X. Zhou, H. Shi, B. Zhang, X. Fu, K. Jiao, Facile synthesis and electrochemical application of surface-modified Bi_2S_3 urchin-like nano-spheres at room temperature, Mat. Lett. 62 (2008) 3201–3204.

[40] X. Meng, Z. Xu, M. Wang, H. Yin, S. Ai, Electrochemical behavior of antipyrine at a Bi_2S_3 modified glassy carbon electrode and its determination in pharmaceutical formulations, Anal. Methods 4 (2012) 1736–1741.

[41] Y. Xu, G. Li, J. Liu, G. Chen, Hierarchical chlorophytum-like Bi_2S_3 architectures with high electrochemical performance, Int. J. Hydrogen Energy 38 (2013) 9137–9144.

[42] E.K. Ylhäinen, M.R. Nunes, A.J. Silvestre, O.C. Monteiro, Synthesis of titanate nanostructures using amorphous precursor material and their adsorption/photocatalytic properties, J. Mater. Sci. 47 (2012) 4305–4312.

[43] O.C. Monteiro, H.I.S. Nogueira, T. Trindade, M. Motevalli, Use of dialkyldithiocarbamato complexes of bismuth(III) for the preparation of nano- and microsized Bi_2S_3 particles and the X-ray crystal structures of $[Bi\{S_2CN(CH_3)(C_6H_{13})\}_3]$ and $[Bi\{S_2CN(CH_3)(C_6H_{13})\}_3(C_{12}H_8N_2)]$, Chem. Mater. 13 (2001) 2103–2111.

[44] Y.P. Dong, L. Huang, J. Zhang, X.F. Chu, Q.F. Zhang, Electro-oxidation of ascorbic acid at bismuth sulfide nanorod modified glassy carbon electrode, Electrochim. Acta 74 (2012) 189–193.

[45] S. Song, A. Song, J. Hao, Hexagonal hollow microtubes incorporated Bi_2S_3-quantum-dots for catalytic degradation of dyes, J. Colloid Interf. Sci. 413 (2014) 133–139.

[46] F. Li, J. Li, Y. Feng, L. Yang, Z. Du, Electrochemical behavior of graphene doped carbon paste electrode and its application for sensitive determination of ascorbic acid, Sens. Actuators B 157 (2011) 110–114.

[47] V.C. Ferreira, O.C. Monteiro, Synthesis and properties of Polythionine/Co-doped titanate nanotubes hybrid materials, Electrochim. Acta 113 (2013) 817–824.

[48] S. Yilmaz, M. Sadikoglu, G. Saglikoglu, S. Yagmur, G. Askin, Determination of ascorbic acid in tablet dosage forms and some fruit juices by DPV, Int. J. Electrochem. Sci. 3 (2008) 1534–1542.

[49] M. Zidan, T.W. Tee, A.H. Abdullah1, Z. Zainal, G.J. Kheng, Electrochemical oxidation of ascorbic acid mediated by Bi_2O_3 microparticles modified glassy carbon electrode, Int. J. Electrochem. Sci. 6 (2011) 289–300.

[50] M.G. Hosseini, M. Faraji, M.M. Momeni, Application of titanium oxide nanotube films containing gold nanoparticles for the electroanalytical determination of ascorbic acid, Thin Solid Films 519 (2011) 3457–3461.

[51] L. Qian, Q. Gao, Y.H. Song, Z. Li, X.R. Yang, Layer-by-layer assembled multilayer films of redox polymers for electrocatalytic oxidation of ascorbic acid, Sens. Actuators B 107 (2005) 303–310.

[52] X.M. Cao, L.Q. Luo, Y.P. Ding, X.L. Zou, R.X. Bian, Electrochemical methods for simultaneous determination of dopamine and ascorbic acid using cetylpyridine bromide/chitosan composite film-modified glassy carbon electrode, Sens. Actuators B 129 (2008) 941–946.